

Hydrothermally Synthesized NanobioMOFs, Evaluated by Photocatalytic Hydrogen Generation

Tabinda Sattar, Muhammad Athar

Institute of Chemical Sciences, Bahaudin Zakaraya University, Multan, Pakistan

Email: tabindasattarahsan22@gmail.com

How to cite this paper: Sattar, T. and Athar, M. (2017) Hydrothermally Synthesized NanobioMOFs, Evaluated by Photocatalytic Hydrogen Generation. *Modern Research in Catalysis*, 6, 80-99.

<https://doi.org/10.4236/mrc.2017.62007>

Received: January 22, 2017

Accepted: April 12, 2017

Published: April 14, 2017

Copyright © 2017 by authors and Scientific Research Publishing Inc.

This work is licensed under the Creative Commons Attribution International License (CC BY 4.0).

<http://creativecommons.org/licenses/by/4.0/>



Open Access

Abstract

Three new materials, nanobioMOFs (cobalt argeninate, cobalt asparaginate and cobalt glutaminate) have been hydrothermally synthesized. Nano sized morphology of all these materials have been obtained by scanning electron microscopic technique. Mass spectrometric studies of all these materials have been conducted for determination of their molar masses. All these nanobio-MOFs have been found to exhibit photocatalytic hydrogen generation in pure water upon irradiation at wavelengths longer than 650 nm. The amounts of quantum yield of hydrogen generation at 650 nm in water was 4.5%, 4.0% and 3.5% for cobalt argeninate, cobalt asparaginate and cobalt glutaminate respectively. The apparently higher yield of hydrogen generation from these amine functionalized nanobioMOFs can direct to the development of more nano sized functionalized MOFs for water splitting.

Keywords

Nano bioMOFs, Cobalt Argeninate, Cobalt Asparaginate, Cobalt Glutamate, Photo Catalysis, Hydrogen Generation

1. Introduction

An amazing property of metal organic frameworks (MOFs) is in the field of photocatalysis. These materials can be used as successful photo catalysts for the reduction of water to generate hydrogen [1] [2]. Photocatalytic water splitting has become an efficient method to produce any greenhouse gases or other harmful effects on environment [3]. So photocatalysis is a phenomenon of converting the solar energy into chemical energy through some MOFs hydrogen fuel as it is inexpensive and environment-friendly fuel as compared to other depleted and expensive fuels, e.g. oil and other nonrenewable fuels [2] [3]. Other advan-

tages of photocatalytic water splitting are that very inexpensive and renewable source as water is used and moreover it doesn't produce materials [4] [5] [6].

In 2010 two zirconium based MOFs, (UiO-66: $Zr_6O_4(OH)_4$ (terephthalic acid)₁₂ and NH_2 -UiO-66: $Zr_6O_4(OH)_4$ (aurintricarboxylic acid)₁₂) have been reported [7] [8]. These two MOFs showed their photocatalytic hydrogen generation under uv irradiation ($\lambda > 300$ nm). As compared to unfunctionalized MOF material UiO-66- NH_2 , the amine functionalized MOF material UiO-66- NH_2 showed slightly better hydrogen production. It has been investigated through experiments that amine functionalization of MOFs can extend the light absorption to the visible region [9]. Although the results of photocatalytic hydrogen production from both of these materials were not too good, it provided an initiative step towards the modification of structure of MOFs for their successful usage for the photocatalytic hydrogen production. Latter on two modified MOFs such as UiO-66/CdS/1% (a reduced graphene oxide ternary composite) and Pt-UiO-66 (anRhodamine B-sensitized) [10] were synthesized from the parent UiO-66 and were used for the more improved catalytic activities for hydrogen production under visible light [11].

Following the strategy of amine functionalization of the MOFs, Matsuoka *et al.* also have synthesized the NH_2 -Ti-MOF. In this material the triethanolamine played a vital role as sacrificial electron donor for photocatalysis under visible light irradiation [12]. A linker to metal charge transfer (LCCT) was observed by the excitation of electron from BDC- NH_2 to the titanium oxo cluster. The authors also have demonstrated that Pt/ NH_2 -Ti-MOF showed a better hydrogen production under visible light but Pt/ NH_2 -Zr-MOF has shown no hydrogen production although it is a visible light adsorbent. The negative CB edge of zirconium oxo cluster as compared to titanium oxo cluster is the main reason of its inactivity to produce hydrogen as there is insufficient supply of electron from organic ligand to zirconium oxo cluster. So conduction band potential of linker molecules is of importance for the photocatalytic hydrogen generation from a MOF material [13].

A Ru-incorporated Ti-based MOF, Ti-MOF-Ru(tpy)₂ has been synthesized by the Matsuoka and co-workers. This material has been investigated to show a better catalytic behavior up to a visible light adsorption of 620 nm (TEOA was used as a sacrificial electron donor) [14]. In 2012 Rosseinskys group have synthesized two MOF materials in which EDTA (ethylene diamine tetra acetic acid) act as a sacrificial electron donor. Both these materials have shown more efficient photocatalytic hydrogen generation under visible light irradiation [15] [16] [17]. In 2013 Xu *et al.* have synthesized two MOF materials, MOF-253 and Pt-MOF-253. Experiments showed that Pt-MOF-253 showed much better catalytic activity to produce hydrogen under visible light adsorption as compared to parental MOF-253 (Here TEOA act as a sacrificial electron donor) But one main disadvantage of using the platinum as a co-catalyst was that the repeat process under visible light reduced the amount of hydrogen produced to nearly half of the actual production [18] [19] [20]. Some nanostructured hybrid shells of

r-GO/AuNP/*m*-TiO₂ have been reported, which showed photocatalytic activity by degradation of Rhodamine B (RhB) under the irradiation of UV [21]. A new hybrid and robust heterogeneous composite material system, Co@MOF has been reported by Nasalevich *et al.* [22]. The light driven hydrogen evolution from water under visible light illumination has been conducted through this material. A composite of the metal-organic framework (MOF) NH₂-MIL-125(Ti) and ionic nickel(II) species has also been reported, which is capable to catalyze hydrogen evolution from water under UV light [23]. Some highly stable zirconium/hafnium-based MOFs were recently introduced and nowadays represent a rapidly growing family. Their unique and intriguing properties make them privileged materials and outstanding candidates in heterogeneous catalysis [24].

From repeated experiments on photocatalysis of MOFs, some points are well to be noted that in order to get more improved photocatalytic activity of MOFs two strategies may be adopted [25]. One is the use of rational design of MOFs and other is the use of co-catalyst. Although the use of a co-catalyst in photocatalysis of MOFs can increase the photocatalytic hydrogen production to many folds but on repeating the process the amount can decrease to a greater extent. So the only useful strategy for better photocatalytic activity is the amine functionalization of the MOFs [26]. The presence of amino group in designing of MOF can't only increase the photocatalytic hydrogen production but also can sustain it for several repeated experiments [27].

The present work describes the hydrothermal synthesis of three new nano sized MOFs. These three materials have been synthesized from three amino acids namely arginine, asparagine and glutamine along with a metal (cobalt). These three materials have been structurally evaluated through scanning electron microscopy (SEM). Mass spectrometry has been conducted to know the molar masses of these nano-sized hybrid materials. Photocatalytic hydrogen productions from all these materials have been carried out under visible light irradiations. TGA and PXRD patterns for all these materials have also been recorded.

2. Experimental

Three new nanobioMOFs have been synthesized by hydrothermal method. Structural morphology of these new materials was determined on S-3400 N scanning electron microscope. AB Sciex 3200 Qtrap mass spectrometer was used for measuring the molecular masses of these materials. Thermogravimetric analysis was performed on SDT Q600, thermo gravimetric instrument. FT-IR spectra were obtained on Shimadzu 8400 FT-IR by preparing KBr pellets. Powder XRD Patterns were recorded on Bruker D₂ Phaser. Photo current experiments were performed on a Pyrex glass reactor.

2.1. Synthesis of Cobaltargininate

Cobalt argeninate has been synthesized by the hydrothermal method. CoCl₂·6H₂O (0.3 g, 0.22 mmol) and arginine (0.4 g, 0.22 mmol) were dissolved in wa-

ter (10 mL). pH of solution was maintained at 10 with the help of Na_2CO_3 . And the solution was heated inside an autoclave at 120°C for 48 hours. After this time, the autoclave was cooled to room temperature in air (natural cooling). The recovered pink colored solid was saved for the photocatalytic reactions and other characterizations.

Elemental analysis: $[\text{Co}(\text{C}_6\text{H}_{13}\text{N}_4\text{O}_2)_2(\text{H}_2\text{O})]$ (423.0) calcd (%) for: Co = 13.94, C = 34.04, H = 6.61, N = 26.48; found: Co = 13.92, C = 34.02, H = 6.60, N = 26.40.

FT-IR spectra of $[\text{Co}(\text{C}_6\text{H}_{13}\text{N}_4\text{O}_2)_2(\text{H}_2\text{O})]$: (4000 - 400 CM^{-1}), 3489.9(br), 3260.7(s), 3070.7(s), 2830.8(m), 1450.8(m), 1330.8(s), 1280.8(s), 990.5(s), 505.4(s).

2.2. Synthesis of Cobalt Asparaginate

Cobalt asparaginate has been synthesized by the hydrothermal method. $\text{CoCl}_2 \cdot 6\text{H}_2\text{O}$ (0.3 g, 0.22 mmol) and asparagines (0.3 g, 0.22 mmol) were dissolved in water (10 mL). All other steps followed were same as given for synthesis of cobalt argeninate.

Elemental analysis: $[\text{Co}(\text{C}_4\text{H}_7\text{N}_2\text{O}_3)_2(\text{H}_2\text{O})]$ (339.0) calcd (%) for: Co = 17.40, C = 28.31, H = 5.01, N = 16.51; found: Co = 17.35, C = 28.29, H = 4.99, N = 16.47.

FT-IR spectra of $[\text{Co}(\text{C}_4\text{H}_7\text{N}_2\text{O}_3)_2(\text{H}_2\text{O})]$: (4000 - 400 CM^{-1}), 3540.5(br), 3345.7(m), 3180.9(s), 2760.4(br), 1488.6(br), 1390.8(s), 1310.5(br), 1150.9(m), 540.6(s).

2.3. Synthesis of Cobalt Glutamate

Cobalt glutamate has been synthesized by the hydrothermal method. $\text{CoCl}_2 \cdot 6\text{H}_2\text{O}$ (0.3 g, 0.22 mmol) and argentine (34 mg, 0.227 mmol) were dissolved in water (10 mL). All other steps were followed as given for synthesis of cobalt argeninate.

Elemental analysis: $[\text{Co}(\text{C}_5\text{H}_9\text{N}_2\text{O}_3)_2(\text{H}_2\text{O})]$ (367.0) calcd (%) for: Co = 16.09, C = 32.79, H = 5.19, N = 15.30; found: Co = 16.05, C = 32.74, H = 5.16, N = 15.25.

FT-IR spectra of $[\text{Co}(\text{C}_5\text{H}_9\text{N}_2\text{O}_3)_2(\text{H}_2\text{O})]$: (4000 - 400 CM^{-1}), 3689.9(br), 3472.7(s), 3180.6(s), 2899.9(m), 1410.5(s), 1280.8(s), 1150.6(s), 830.4(s), 515.4(s).

2.4. Photocatalytic Reactions

A 50 mL Pyrex glass reactor was used to perform the photocatalytic experiments. To measure the evolved hydrogen gas an inverted burette filled with water at atmospheric pressure was connected to the headspace of Pyrex reactor. Then pink colored powder of cobalt argeninate (50 mg) was dispersed in water (30 mL), hence the total volume of the suspensions measured was 30.5 mL. To remove the dissolved air an argon flow was passed through the suspensions nearly half an hour before the irradiation. A tungsten halogen lamp was used to irradiate the suspensions for about two hours continuously, while keeping the glass

reactor at 35°C. By using a semi-capillary column (molecular sieve, 530 mm diameter, 15 m length, equipped with a thermal conductivity detector) nearly 1 mL of the gas produced in the reactor head space was injected into a Hewlett Packward HP 5890 gass chromatograph, operating at isothermal conditions (50°C). At 680 nm visible light irradiation, a photon flux was determined by Meso-diphenylhelianthreneactinometry and a value 12.5×10^{-5} mmol photon s^{-1} was obtained.

In order to know the amount of hydrogen evolved directly from irradiation of pure water, water/methanol and pure methanol, some experiments were performed in the absence of any catalyst (blank experiments). Then these obtained values from the blank experiments were compared with all those obtained in the presence of catalyst (nanobioMOFs).

3. Results and Discussions

Three new nano sized materials have been hydrothermally synthesized and characterized by scanning electron microscopy for determination of morphology and mass spectrometric studies for the assessment of molecular masses. Photocatalytic hydrogen productions from these nanosizedbioMOFs have been carried out. Powder X-rays diffraction studies and thermogravimetric studies of these nano sized materials have also been conducted.

N₂ adsorption measurements of all the thre new nanobioMOF was carried out both in pure form and after photocatalytic reaction in order to evaluate the pore structures and specific surface areas of the materials. The specific surface areas of cobalt argeninate, cobalt asparaginate and cobalt glutamate were determined to be 1235, 1230 and 1220 $m^2 \cdot g^{-1}$, respectively by using BET-method-based calculations on N₂ adsorption isotherm data. It was noted from these findings that all these nanobioMOFs have large specific surface areas associated with their nano porous structures. It was also elaborated that some pores were blocked after the photocatalytic reactions thus decreasing the specific surface areas of these materials to 1020, 995 and 990 $m^2 \cdot g^{-1}$, respectively.

3.1. Scanning Electron Microscopic (SEM) Studies of NanobioMOFs

S-3400N Scanning electron microscope was used to obtain the images of all three nano materials (cobalt argeninate, cobalt asparaginate and cobalt glutamate) which revealed the formation of nano sized structures (plates and rodes) of these materials. So in this manner nanobioMOF formation has been evaluated by the scanning electron micrographic images of these materials.

For SEM all samples of appropriate sizes were generally mounted rigidly on a specimen holder called a specimen stub. The electron beam, having an energy ranging from 0.2 keV to 40 keV, by one or two condenser lenses is focused to a spot about 0.4 nm to 5 nm in diameter. The beam current absorbed by the specimen was used to create images of the distribution of specimen current. From a high-resolution cathode ray tube the microscopes images were captured, digi-

tized and saved as digital images.

SEM image of a material “cobalt argeninate” is represented in **Figure 1** which indicates the formation of nano sized block like structures of the material. Whereas the **Figure 2** and **Figure 3** describe the formation of nano sized plate like structures of the materials, cobalt asparaginate and cobalt glutamate.

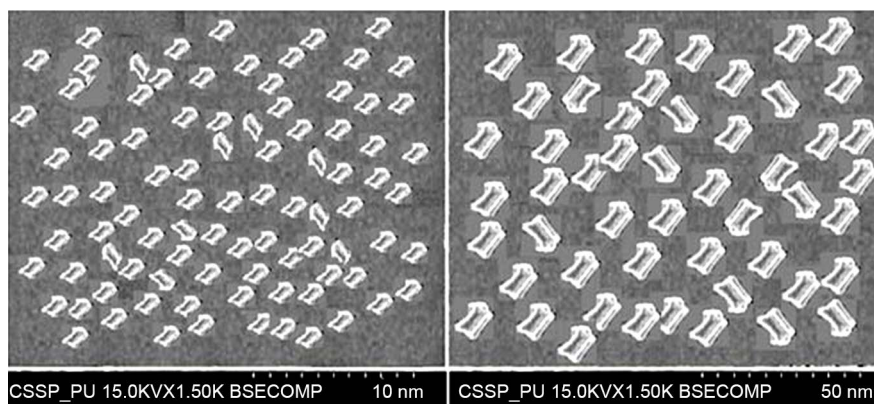


Figure 1. SEM images of “cobalt argeninate” showing the formation of nano sized block like structures of the material.

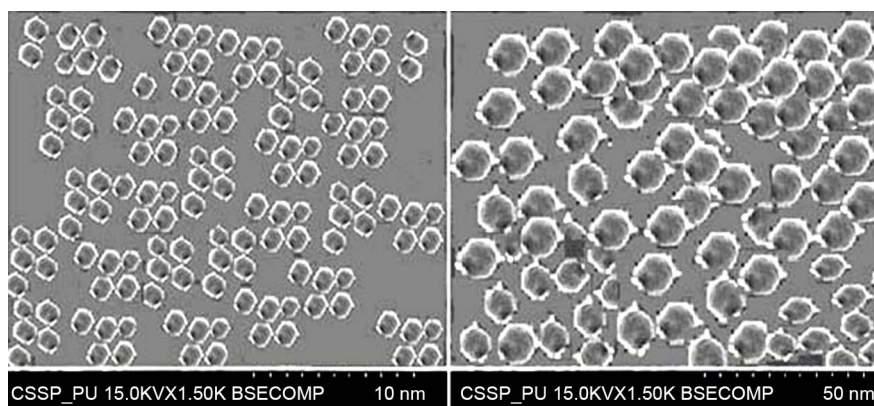


Figure 2. SEM images of “cobalt argeninate” showing the formation of nano sized plate like structures of the material.

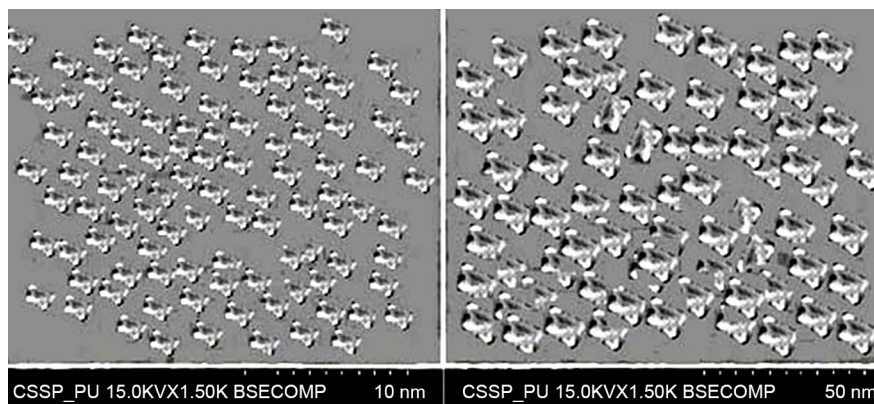


Figure 3. SEM images of “cobalt glutamate” showing the formation of nano sized plate like structures of the material.

3.2. Mass Spectrometric Studies of NanobioMOFs

The molecular masses of “cobalt argeninate”, “cobalt asparaginate” and “cobalt glutamate” have been determined by AB Sciex 3200 Qtrap mass spectrometer. Spectra were obtained by adding together the transient signals recorded from 50 to 200 laser shots using a CAMAC crate based transient recorder and crate controller. The summed spectrum was transferred to a VAXWorkstation 3200 for data analysis.

In a typical MS procedure all solid samples were ionized by bombarding them with electrons, some of the sample’s molecules to break into charged fragments as a result of this bombardment. According to their mass-to-charge ratio, these ions were then separated, typically by accelerating them and subjecting them to an electric or magnetic field. A mechanism capable of detecting charged particles, such as an electron multiplier was used to detect the ions. Spectra of the relative abundance of detected ions as a function of the mass-to-charge ratio were displayed as results. Mass spectra of all the three nanobioMOFs (cobalt argeninate, cobalt asparaginate and cobalt glutamate) are given below as **Figure 4**, **Figure 5** and **Figure 6** respectively. Whereas the theoretical and experimental values of molecular masses of cobalt argeninate, cobalt asparaginate and cobalt glutamate have been given in **Table 1**, **Table 2** and **Table 3** respectively.

Table 1. Measured and calculated molecular masses of cobalt argeninate.

Molecular formula	[M+H] ⁺	Average measured mass(u)	Calculated mass(u)	Difference
	423.06			
[Co(C ₆ H ₁₃ N ₄ O ₂) ₂ (H ₂ O)]	423.05	423.05	423.00	0.05
	423.04			

Table 2. Measured and calculated molecular masses of cobalt asparaginate.

Molecular formula	[M+H] ⁺	Average measured mass(u)	Calculated mass(u)	Difference
	339.06			
[Co(C ₄ H ₇ N ₂ O ₃) ₂ (H ₂ O)]	339.05	338.05	338.00	0.05
	339.04			

Table 3. Measured and calculated molecular masses of cobalt glutamate.

Molecular formula	[M+H] ⁺	Average measured mass(u)	Calculated mass(u)	Difference
	367.06			
[Co(C ₅ H ₉ N ₂ O ₃) ₂ (H ₂ O)]	367.05	367.05	367.00	0.05
	367.04			

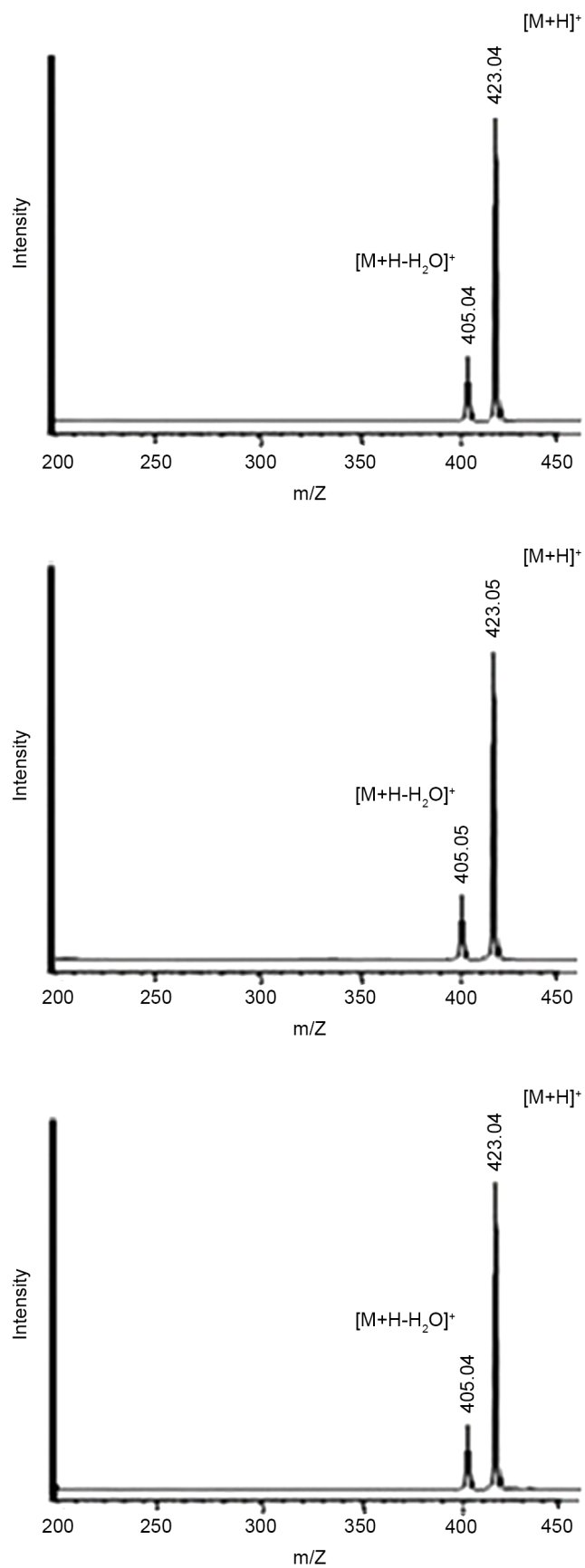


Figure 4. Mass spectra of cobalt argeninate.

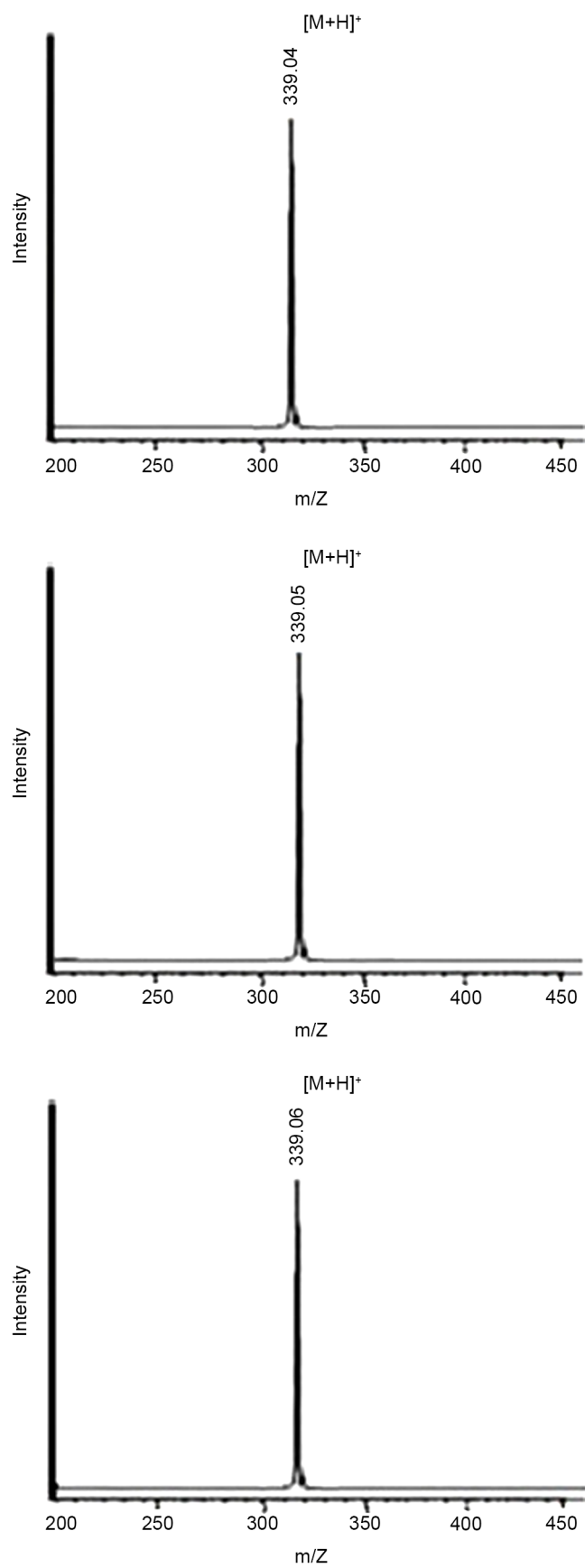


Figure 5. Mass spectra of cobalt asparaginate.

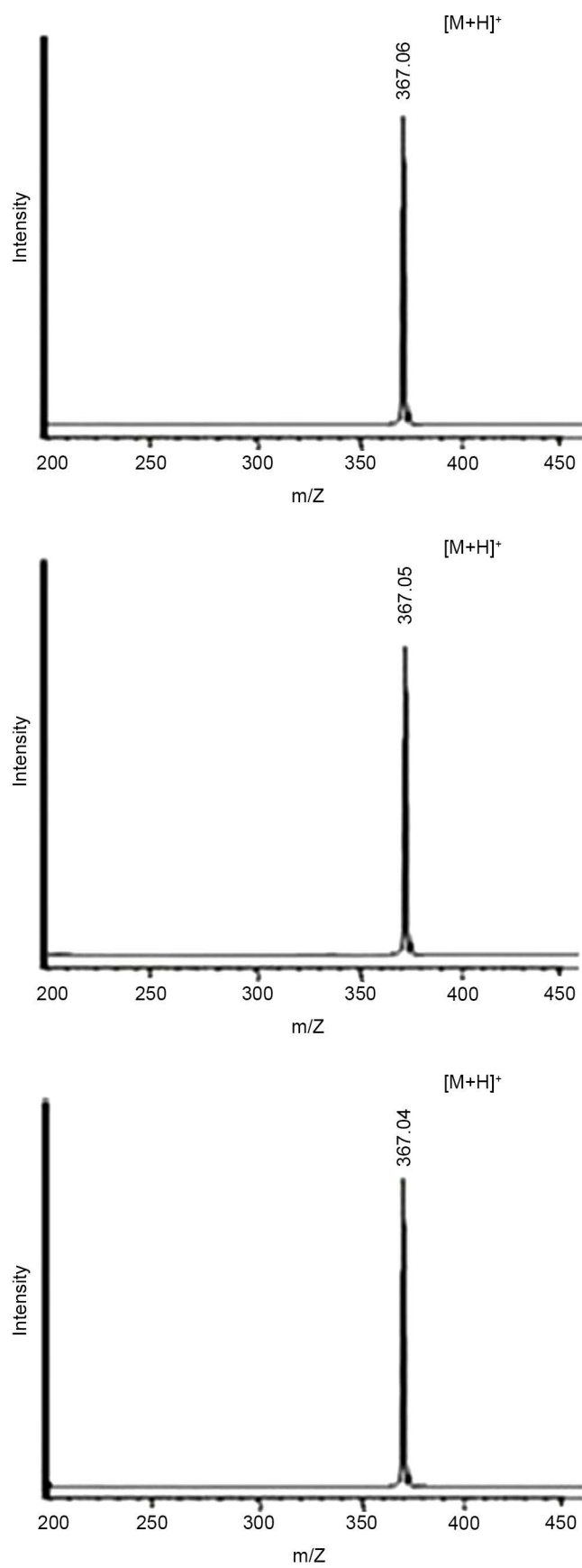


Figure 6. Mass spectra of cobalt glutamate.

3.3. Thermogravimetric Studies of NanobioMOFs

SDT Q600 thermo gravimetric analyzer was used to record the thermograms of cobalt argeninate, cobalt asparaginate and cobalt glutamate. All these compounds were heated separately from 0°C to 600°C at a heating rate of 10°C per minute. The plot of cobalt argeninate shows a first weight loss of nearly 10% at 130°C which is due to the loss of coordinated water molecules in these compounds. Then up to 370°C the framework shows stability without further weight loss. After 370°C the decomposition of whole frameworks is observed which is completed beyond 400°C with maximum weight loss of 68%. The plot of cobalt asparaginate indicates a first weight loss of nearly 10% at 130°C which is due to the loss of coordinated water molecules in this compound. Then up to 330°C the framework shows stability without further weight loss. After 330°C the framework starts its decomposition slowly and gradually until the whole framework is decomposed up to 400°C with maximum weight loss of 69%.

The plot of cobalt glutamate shows a first weight loss of nearly 8% at 155°C which is due to the loss of coordinated water molecules. Then up to 350°C the framework remains stable without further weight loss. After 350°C the decomposition of whole framework is observed which is completed beyond 380°C with maximum weight loss of 65%. **Figure 7** represents the thermograms of the three newly synthesized nano sized materials.

3.4. Photoelectro Chemical Measurements

Photoelectro chemical measurements of all the newly synthesized materials were carried out on a photo electrochemical test system which was composed of a HZ3000 potentiostat (Hokuto Denko), a tungsten lamp with an appropriate cutoff filter and two-electrode cell with saturated calomel electrode (SCE) as the reference electrode and nanobioMOFs (cobalt argeninate) as the working electrode. 0.25 M K_2SO_4 aqueous solutions containing 0.01 M TEOA was used as the electrolytic solution. The nanobioMOFs electrode was synthesized by depositing a suspension made of nanobioMOF and methanol onto an indium-tin-oxide-coated polyethylene naphthalate (ITO-PEN) film with the help of a coating method after that it was dried at 373 K for a time period of one hour. By monitoring the photocurrent signal produced by a light irradiation the spectral response of the nanobioMOF electrode was measured through an appropriate cutoff filter under a constant potential of 0.5 V versus saturated calomel electrode (SCE).

3.5. Photocatalytic Hydrogen Production by NanobioMOFs

All the three nanobioMOFs were tested for the photocatalytic hydrogen production. Different experiments were performed to know the effect of UV light irradiation on cobalt argeninate, cobalt asparaginate and cobalt glutamate suspensions in water and also in methanol. But no detectable amounts of hydrogen were produced under UV light irradiations. Also the amount of hydrogen produced by the visible light irradiation of three nanobioMOFs suspensions in water/methanol was comparatively less than the amount of hydrogen produced by the

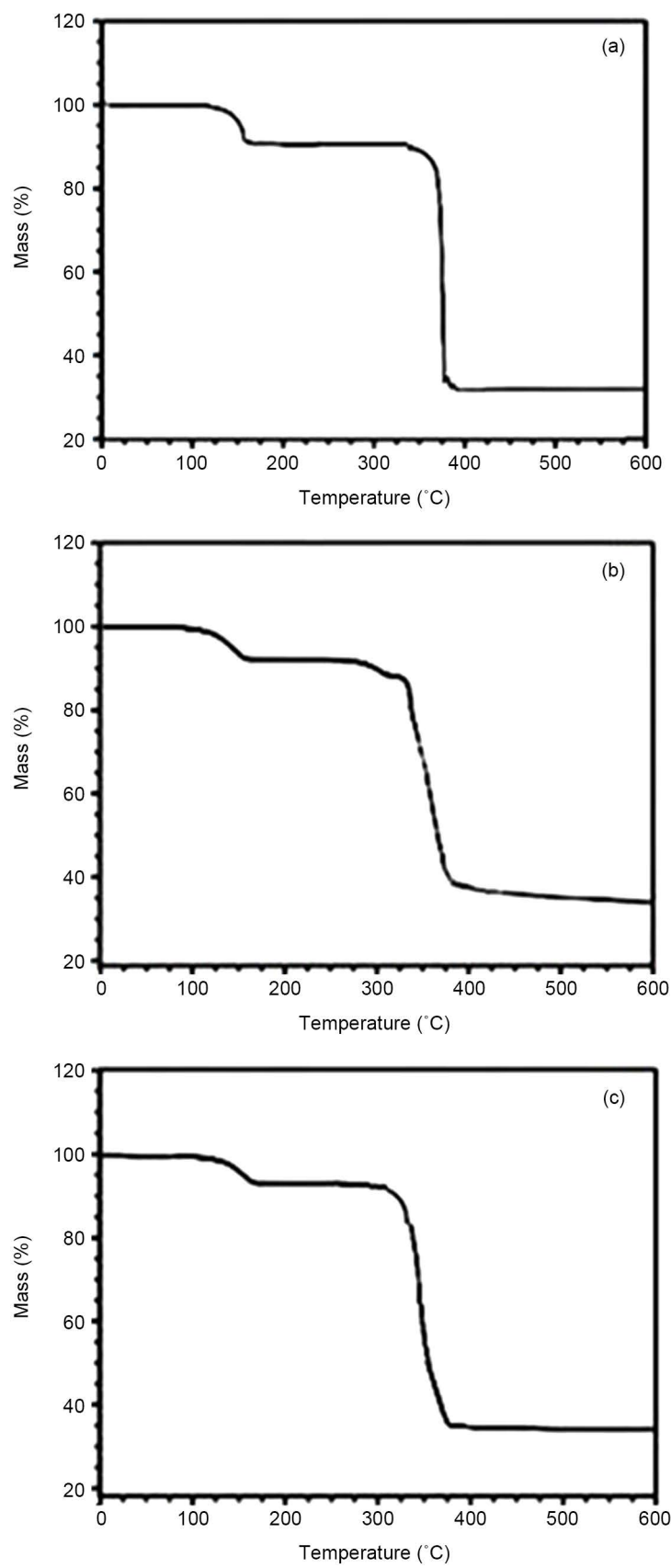


Figure 7. TGA plot of (a) cobalt argeninate, (b) cobalt asparaginate, (c) cobalt glutamate.

visible light irradiation of these materials suspensions in water alone. So it can be concluded from these experiments that amine functionalized MOF (cobalt argeninate) can itself act as a stronger sacrificial electron donor being the source of the electrons required in the reduction semi-reaction of water as compared to methanol. UV/Vis spectra of all the three materials cobalt argeninate, cobalt asparaginate and cobalt glutamate are given following as **Figure 8**.

These new materials actually act as semiconductor type materials for the photocatalytic production of hydrogen. Some examples are present in literature in which cobalt based MOFs have been used for photocatalytic dye degradation that indicate that the UV irradiation resulted in charge separation with electrons in LUMO (lowest unoccupied molecular orbital) and electron holes in HOMO (Highest occupied molecular orbital). So in order to elaborate the phenomenon of charge separation in cobalt argeninate, cobalt asparaginate and cobalt glutamate a laser flash photolysis was used to detect the states of charge separation which are characteristics of semiconductors. Different volumes of hydrogen gas evolved by using pure water, pure methanol and different proportions of water and methanol for cobalt argeninate, cobalt asparaginate and cobalt glutamate are given as **Figure 9**.

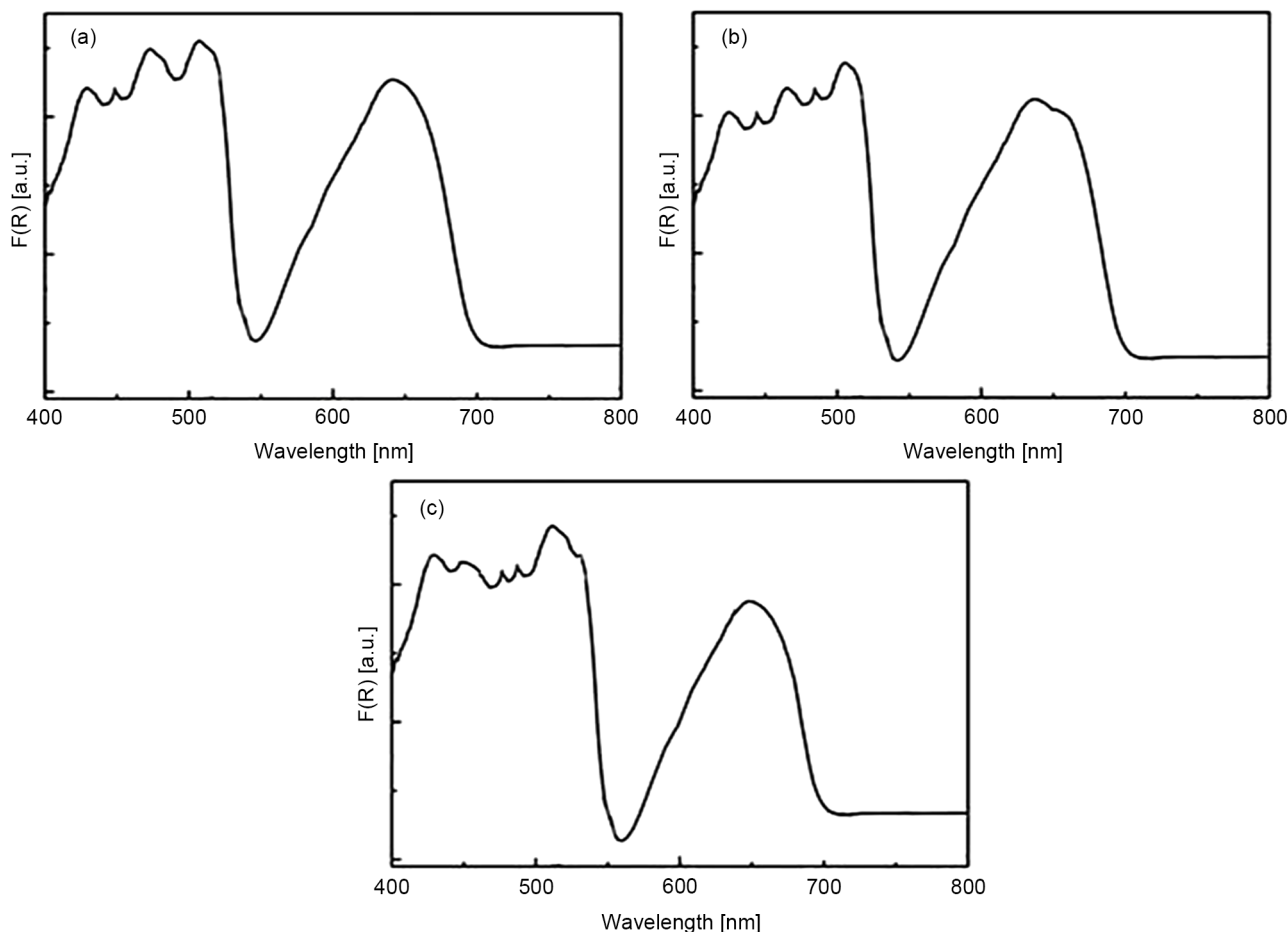


Figure 8. (a) UV/Vis spectra of cobalt argeninate, (b) UV/Vis spectra of cobalt asparaginate, (c) UV/Vis spectra of cobalt glutamate.

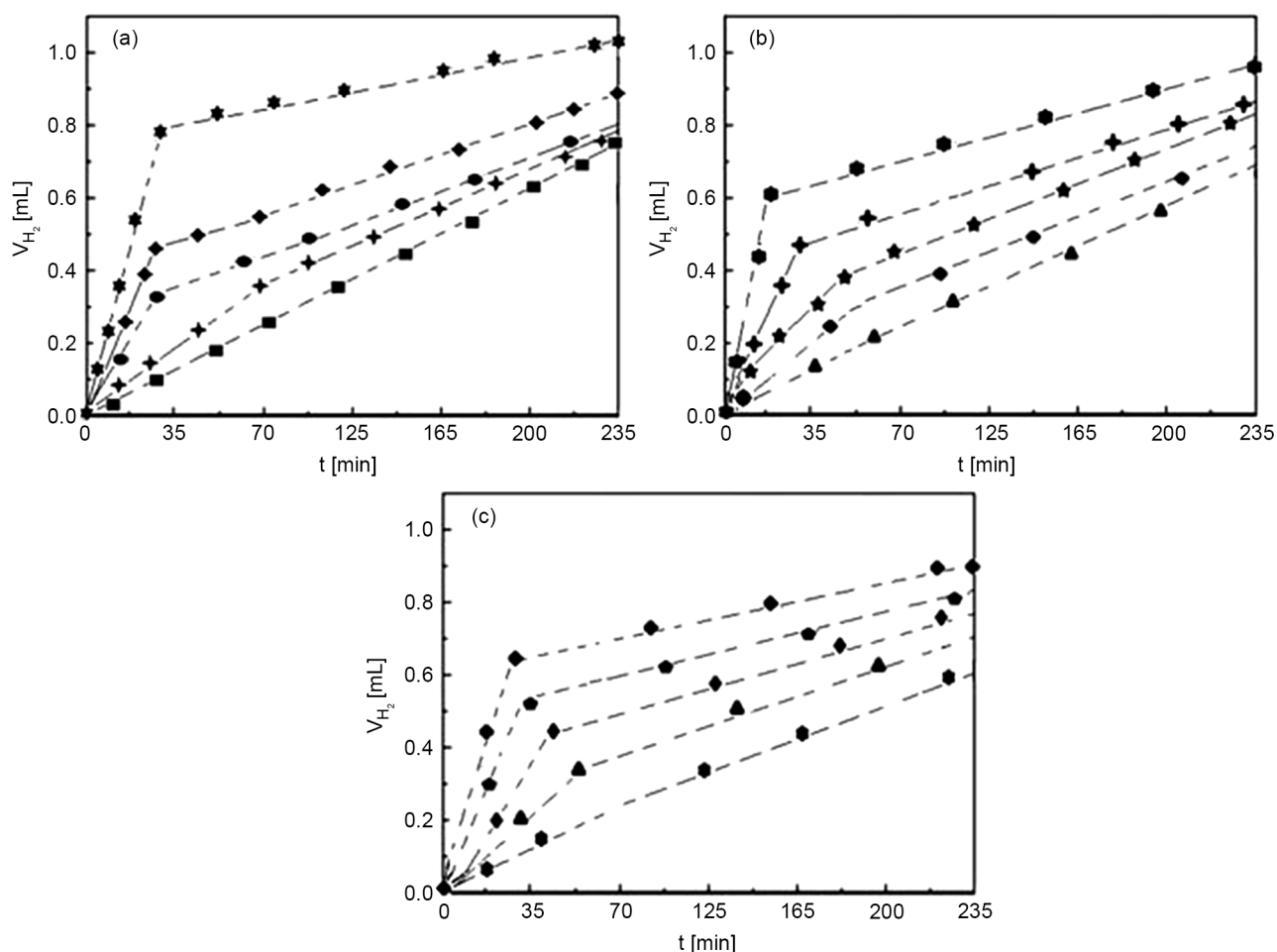


Figure 9. (a) Volume of hydrogen evolved (V_{H_2}) during the photocatalytic reactions of cobalt argeninate, using pure water (★) 50% water: 50% methanol (◆) 30% water: 50% methanol (●), 10% water: 90% methanol (✦), pure methanol (■), (b) Volume of hydrogen evolved (V_{H_2}) during the photocatalytic reactions of cobalt asparaginate, using pure water (★) 50% water: 50% methanol, (✦) 30% water: 50% methanol (★), 10% water: 90% methanol (●), pure methanol (▲) (c) Volume of hydrogen evolved (V_{H_2}) during the photocatalytic reactions of cobalt glutamate, using pure water (◆) 50% water: 50% methanol (●) 30% water: 50% methanol (●), 10% water: 90% methanol (▲), pure methanol (●).

3.6. Reaction Mechanism of Photocatalytic Hydrogen Generation

In situ ESR measurements were carried out after visible-light irradiation for all the three nano sized materials and these results indicate that LCCT mechanism is followed in the photocatalytic process. All newly synthesized materials were immersed in a solution of 0.01 M aqueous TEOA, and the suspension was evacuated at 77 K. Then these materials were irradiated at room temperature by visible light ($\lambda > 420$ nm) for a time period of nearly 3 hours. After the irradiation of these samples their ESR spectra were recorded at 77 K. The signals of ESR spectrum after visible light irradiation were found to have parameters that are characteristic of paramagnetic Co^{2+} centers in a distorted rhombic oxygen ligand field ($g_x = 2.125$, $g_y = 2.118$, and $g_z = 2.105$ for cobalt argeninate; $g_x = 2.123$, $g_y = 2.115$, and $g_z = 2.110$ for cobalt asparaginate; $g_x = 2.121$, $g_y = 2.115$, and $g_z = 2.101$ for cobalt glutamate). From these results it has been elaborated that in all these nanobioMOFs, visible light promotes transfer of photo generated electrons

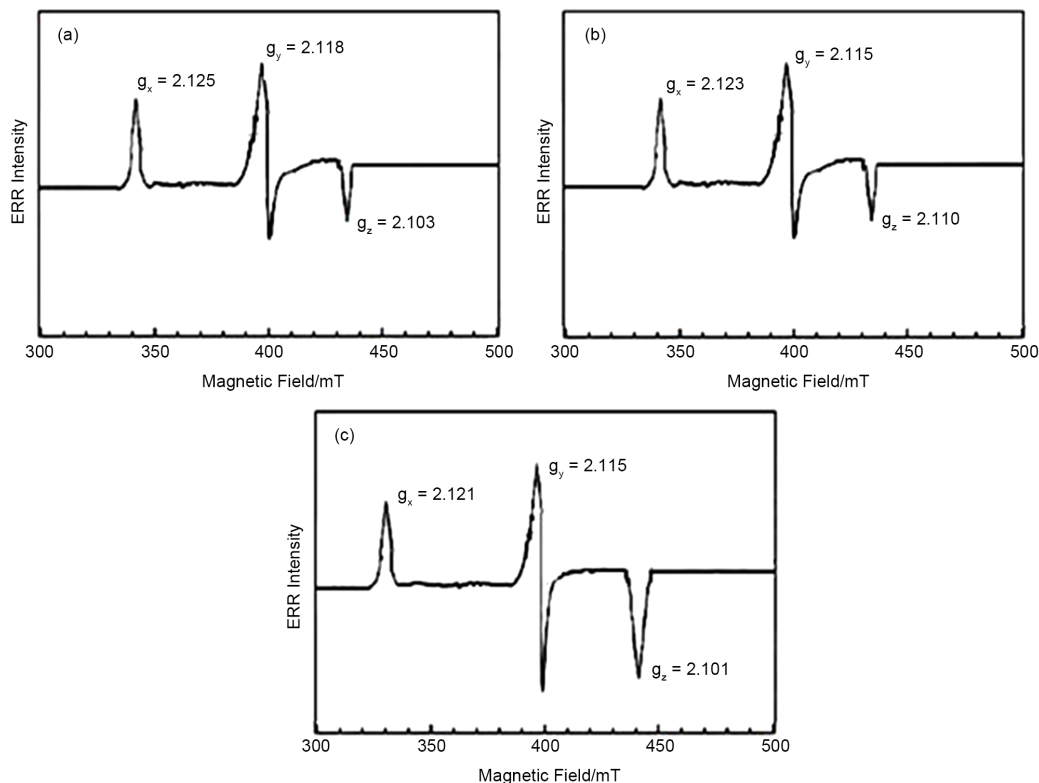


Figure 10. ESR spectra of (a) cobalt argeninate, (b) cobalt asparaginate, (c) cobalt glutamate.

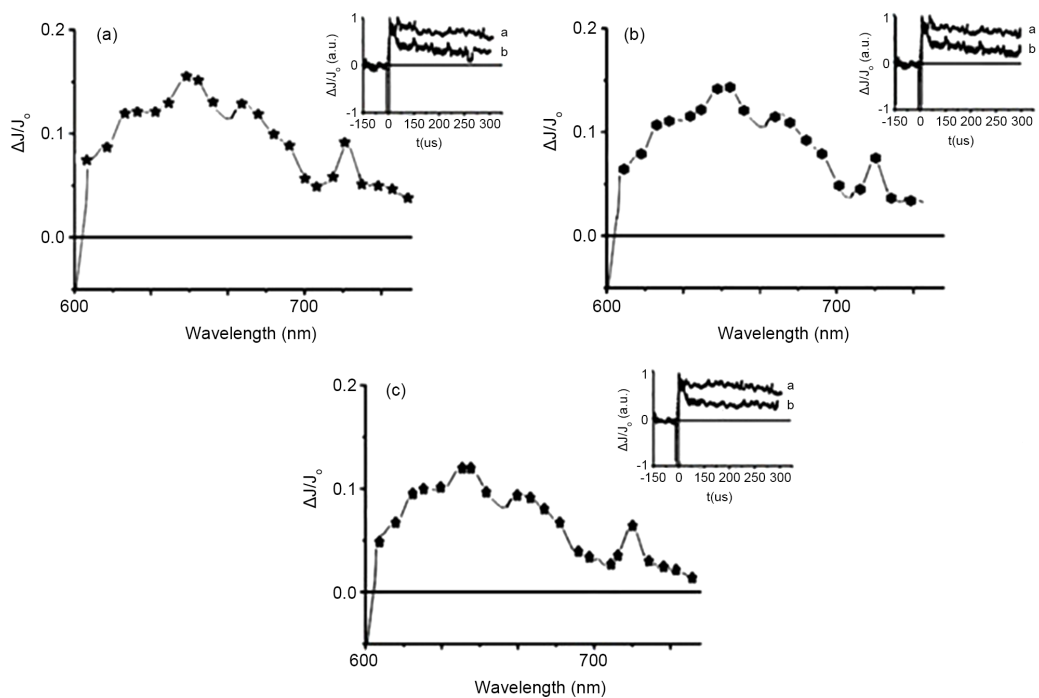


Figure 11. (a) Time-resolved transient spectra recorded 9.5 ms after the laser flash corresponding to cobalt argeninate. Inset: Temporal profiles of the transient spectrum of cobalt argeninate monitored at (a) 650 and (b) 700 nm, (b) Time-resolved transient spectra recorded 9.5 ms after the laser flash corresponding to cobalt asparaginate, Inset: Temporal profiles of the transient spectrum of cobalt asparaginate monitored at (a) 650 and (b) 700 nm, (c) Time-resolved transient spectra recorded 9.5 ms after the laser flash corresponding to cobalt glutamate, Inset: Temporal profiles of the transient spectrum of cobalt glutamate monitored at (a) 650 and (b) 700 nm.

from the excited $\text{NH}_2\text{-R-COOH}$ group to the conduction band of cobalt-oxo cluster which resulted in the formation of Co^{2+} species. EPR spectra of cobalt argeninate, cobalt asparaginate and cobalt glutamate are given below as **Figure 10**.

Transient spectra of cobalt argeninate, cobalt asparaginate and cobalt glutamate were obtained by using a 655 nm laser excitation under N_2 atmosphere. These spectra indicate the continuous absorption from 600 to 700 nm with relative maxima at 650 nm. And the signals of all the transient spectra (**Figure 11**) of three materials do not show a decay even after 300 us (longest lifetime available in nanosecond laser system so indicating that these are long lived).

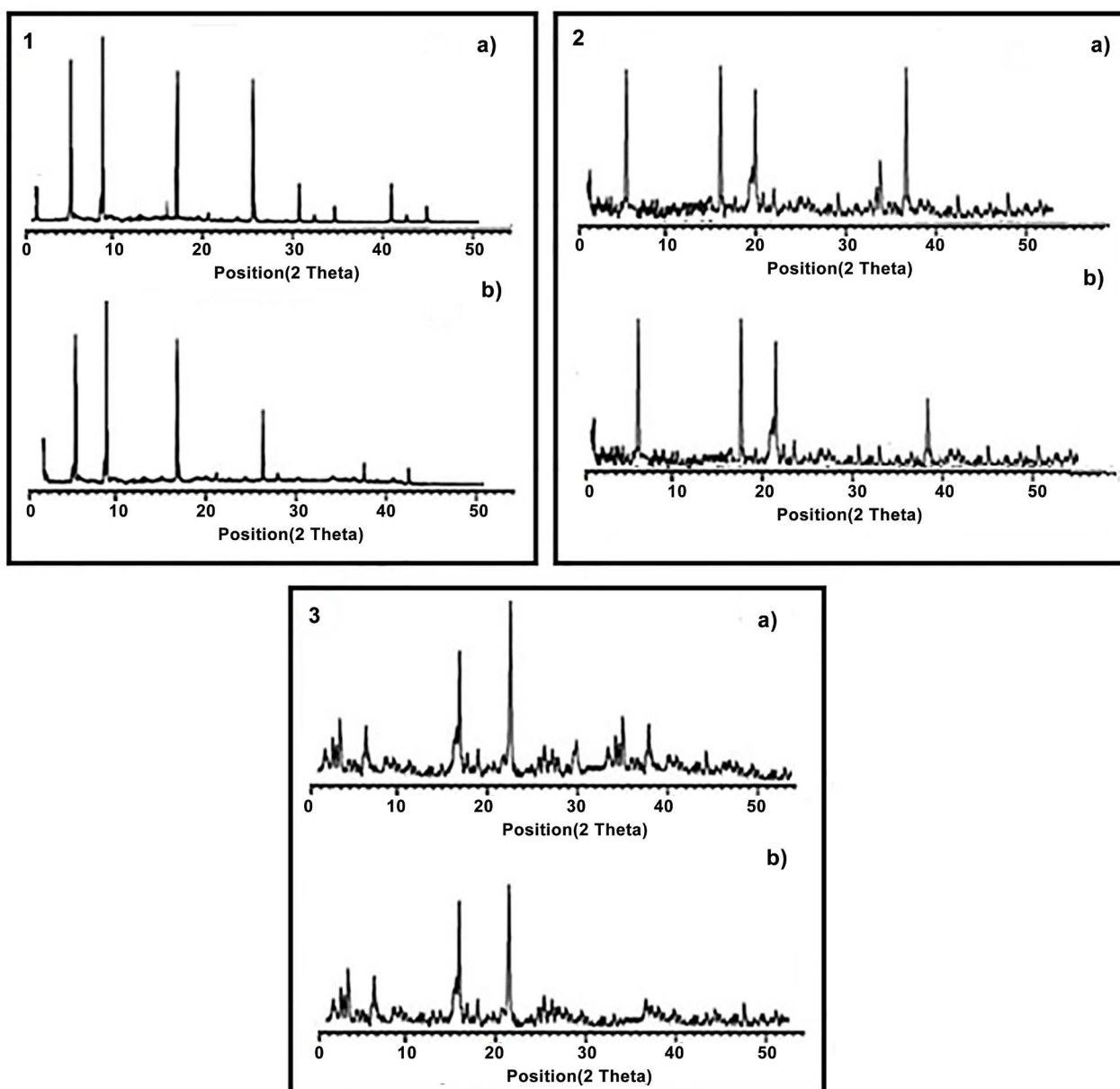


Figure 12. PXRD pattern of 1) cobalt argeninate a) before photocatalytic reaction, b) after photocatalytic reaction, 2) cobalt asparaginate a) before photocatalytic reaction, b) after photocatalytic reaction, 3) cobalt glutamate a) before photocatalytic reaction, b) after photocatalytic reaction.

3.7. Powder X-Rays Diffraction Studies

The X-Rays diffraction patterns of nanobioMOFs, cobalt argeninate, cobaltasparaginate and cobalt glutamate in pure form and after photocatalytic reactions were recorded and compared as given below in **Figure 12**. By comparison of the XRD pattern it was found that the XRD pattern remained nearly unchanged after photocatalytic reactions which indicate that the photodeposition process does not influence the structures of these materials.

4. Conclusions

MOFs possess a great potential as photocatalysts especially for the hydrogen generations. The present work describes the importance of amine functionalized MOFs for photocatalytic hydrogen generation. It has been investigated that the amine functionalized MOFs can exhibit better more photocatalytic hydrogen production especially under visible light irradiations. All the three newly synthesized nano-sized amine functionalized materials have shown much better photocatalytic hydrogen production under visible light irradiations. As the amount of hydrogen produced by these three materials is much higher so the present study can lead to the production of more such nano-sized MOFs materials with amine functionalization for better photocatalytic hydrogen production.

References

- [1] Yadav, R.K., Baeg, J.O., Oh, G.H., Park, N.J., Kong, K.J., Kim, J., Hwang, D.W. and Biswas, S.K. (2012) A Photocatalyst-Enzyme Coupled Artificial Photosynthesis System for Solar Energy in Production of Formic Acid from CO₂. *Journal of the American Chemical Society*, **134**, 11455-11461. <https://www.ncbi.nlm.nih.gov/pubmed/22769600> <https://doi.org/10.1021/ja3009902>
- [2] Berardi, S., Drouet, S., Francas, L., Gimbert-Surinach, C., Guttentag, M., Richmond, C., Stoll, T. and Llobet, A. (2014) Molecular Artificial Photosynthesis. *Chemical Society Reviews*, **43**, 7501-7519. <https://www.ncbi.nlm.nih.gov/pubmed/24473472> <https://doi.org/10.1039/c3cs60405e>
- [3] Cokoja, M., Bruckmeier, C., Rieger, B., Herrmann, W.A., Kühn, F.E., Bruckmeier, C., Rieger, B., Herrmann, W.A. and Kühn, F.E. (2011) Transformation of Carbon Dioxide with Homogeneous Transition-Metal Catalysts: A Molecular Solution to a Global Challenge? *Angewandte Chemie International Edition*, **50**, 8510-8537. <https://www.ncbi.nlm.nih.gov/pubmed/21887758> <https://doi.org/10.1002/anie.201102010>
- [4] Zhang, Y., Tang, Y., Liu, X., Dong, Z., Hng, H.H., Chen, Z., Sum, T.C. and Chen, X. (2013) Three-Dimensional CdS-Titanate Composite Nanomaterials for Enhanced Visible-Light-Driven Hydrogen Evolution. *Small*, **9**, 996. <http://onlinelibrary.wiley.com/doi/10.1002/sml.201202156/full> <https://doi.org/10.1002/sml.201202156>
- [5] Fu, Y., Sun, D., Chen, Y., Huang, R., Ding, Z., Fu, X. and Li, Z. (2012) An Amine-Functionalized Titanium Metal-Organic Framework Photocatalyst with Visible-Light-Induced Activity for CO₂ Reduction. *Angewandte Chemie International Edition*, **51**, 3364-3367. <https://www.ncbi.nlm.nih.gov/pubmed/22359408> <https://doi.org/10.1002/anie.201108357>

- [6] Guo, S., Bao, J., Hu, T., Zhang, L., Yang, L., Peng, J. and Jiang, C. (2015) Controllable Synthesis Porous Ag_2CO_3 Nanorods for Efficient Photocatalysis. *Nanoscale Research Letters*, **21**, 193. <https://www.ncbi.nlm.nih.gov/pubmed/25977664>
<https://doi.org/10.1186/s11671-015-0892-5>
- [7] Jiang, Z., Tang, Y., Tay, Q., Zhang, Y., Malyi, O.I., Wang, D., Deng, J., Lai, Y., Zhou, H., Chen, X., Dong, Z. and Chen, Z. (2013) Understanding the Role of Nanostructures for Efficient Hydrogen Generation on Immobilized Photocatalysts. *Advanced Energy Materials*, **3**, 1368-1380.
<http://onlinelibrary.wiley.com/doi/10.1002/aenm.201300380/ful>
<https://doi.org/10.1002/aenm.201300380>
- [8] Lang, X., Chen, X. and Zhao, J. (2014) Heterogeneous Visible Light Photocatalysis for Selective Organic Transformations. *Chemical Society Reviews*, **43**, 473-486.
<https://www.ncbi.nlm.nih.gov/pubmed/24162830>
<https://doi.org/10.1039/C3CS60188A>
- [9] Cavka, J.H., Jakobsen, S., Olsbye, U., Guillou, N., Lamberti, C., Bordiga, S. and Lillerud, K.P. (2008) A New Zirconium Inorganic Building Brick Forming Metal Organic Frameworks with Exceptional Stability. *Journal of the American Chemical Society*, **130**, 13850-13851. <https://www.ncbi.nlm.nih.gov/pubmed/18817383>
<https://doi.org/10.1021/ja8057953>
- [10] Silva, C.G., Luz, I., Llabrés i Xamena, F.X., Corma, A. and García, H. (2010) Water Stable Zr-Benzenedicarboxylate Metal-Organic Frameworks as Photocatalysts for Hydrogen Generation. *Chemistry: A European Journal*, **16**, 11133-11138.
<http://onlinelibrary.wiley.com/doi/10.1002/chem.200903526/ful>
- [11] Lin, R., Shen, L., Ren, Z., Wu, W., Tan, Y., Fu, H., Zhang, J. and Wu, L. (2014) Enhanced Photocatalytic Hydrogen Production Activity via Dual Modification of MOF and Reduced Graphene Oxide on CdS. *Chemical Communications*, **50**, 8533-8535.
<http://pubs.rsc.org/En/content/articlelanding/2014/cc/c4cc01776e#!divAbstract>
<https://doi.org/10.1039/C4CC01776E>
- [12] Horiuchi, Y., Toyao, T., Saito, M., Mochizuki, K., Iwata, M., Higashimura, H., Anpo M. and Matsuoka M. (2012) Visible-Light-Promoted Photocatalytic Hydrogen Production by Using an Amino-Functionalized Ti(IV) Metal-Organic Framework. *The Journal of Physical Chemistry C*, **116**, 20848-20853.
<http://pubs.acs.org/doi/abs/10.1021/jp3046005>
<https://doi.org/10.1021/jp3046005>
- [13] He, J., Wang, J., Chen, Y., Zhang, J., Duan, D., Wang, Y. and Yan, Z. (2014) A Dye-Sensitized Pt UiO-66(Zr) Metal-Organic Framework for Visible-Light Photocatalytic Hydrogen Production. *Chemical Communications*, **50**, 7063.
<http://pubs.rsc.org/EN/content/articlelanding/2014/cc/c4cc01086h#!divAbstract>
<https://doi.org/10.1039/c4cc01086h>
- [14] Toyao, T., Saito, M., Horiuchi, Y., Mochizuki, K., Iwata, M., Higashimura, H. and Matsuoka, M. (2013) Efficient Hydrogen Production and Photocatalytic Reduction of Nitrobenzene over a Visible-Light-Responsive Metal-Organic Framework Photocatalyst. *Catalysis Science & Technology*, **3**, 2092-2097.
<http://pubs.rsc.org/en/content/articlelanding/2013/cy/c3cy00211j#!divAbstract>
<https://doi.org/10.1039/c3cy00211j>
- [15] Wen, M., Mori, K., Kamegawa, T. and Yamashita, H. (2014) Amine-Functionalized MIL-101(Cr) with Imbedded Platinum Nanoparticles as a Durable Photocatalyst for Hydrogen Production from Water. *Chemical Communications*, **50**, 11645-11648.
<http://pubs.rsc.org/En/content/articlelanding/2014/cc/c4cc02994a#!divAbstract>
<https://doi.org/10.1039/C4CC02994A>

- [16] Toyao, T., Saito, M., Dohshi, S., Mochizuki, K., Iwata, M., Higashimura, H., Horiuchi, Y. and Matsuoka, M. (2014) Development of a Ru Complex-Incorporated MOF Photocatalyst for Hydrogen Production under Visible-Light Irradiation. *Chemical Communications*, **50**, 6779-6781. <https://www.ncbi.nlm.nih.gov/pubmed/24836941>
<https://doi.org/10.1039/c4cc02397h>
- [17] Fateeva, A., Chater, P.A., Ireland, C.P., Tahir, A.A., Khimiyak, Y.Z., Wiper, P.V., Darwent, J.R. and Rosseinsky, M.J. (2012) A Water-Stable Porphyrin-Based Metal-Organic Framework Active for Visible-Light Photocatalysis. *Angewandte Chemie International Edition*, **51**, 7440-7444.
<https://www.ncbi.nlm.nih.gov/pubmed/22696508>
<https://doi.org/10.1002/anie.201202471>
- [18] Wang, G., Sun, Q., Liu, Y., Huang, B., Dai, Y., Zhang, X. and Qin, X. (2015) A Bismuth-Based Metal-Organic Framework as an Efficient Visible-Light-Driven Photocatalyst. *Chemistry: A European Journal*, **21**, 2364.
<http://onlinelibrary.wiley.com/doi/10.1002/chem.201405047/abstract>
<https://doi.org/10.1002/chem.201405047>
- [19] Wang, C., Xie, Z. deKrafft, K.E. and Lin, W. (2011) Doping Metal-Organic Frameworks for Water Oxidation, Carbon Dioxide Reduction, and Organic Photocatalysis. *Journal of the American Chemical Society*, **133**, 13445-13454.
<https://www.ncbi.nlm.nih.gov/pubmed/21780787>
<https://doi.org/10.1021/ja203564w>
- [20] Wang, C., Wang, J.L. and Lin, W. (2012) Elucidating Molecular Iridium Water Oxidation Catalysts Using Metal-Organic Frameworks: A Comprehensive Structural, Catalytic, Spectroscopic, and Kinetic Study. *Journal of the American Chemical Society*, **134**, 19895-19908. <https://www.ncbi.nlm.nih.gov/pubmed/23136923>
<https://doi.org/10.1021/ja310074j>
- [21] Wang, M., Han, J., Xiong, H., Rong, G. and Yadong, Y. (2015) Nanostructured Hybrid Shells of r-GO/AuNP/m-TiO₂ as Highly Active Photocatalysts. *ACS Applied Materials & Interfaces*, **7**, 6909-6918.
<http://pubs.acs.org/doi/abs/10.1021/acsami.5b00663?src=recsys>
<https://doi.org/10.1021/acsami.5b00663>
- [22] Nasalevich, M.A., Becker, R., Ramos-Fernandez, E.V., Castellanos, S., Veber, S.L., Fedin, M.V., Kapteijn, F., Reek, J.N.H., van der Vlugt, J.I. and Gascon, J. (2015) Co NH₂-MIL-125(Ti): Cobaloxime-Derived Metal-Organic Framework-Based Composite for Light-Driven H₂ Production. *Energy & Environmental Science*, **8**, 364-375.
<http://pubs.rsc.org/en/content/articlelanding/2015/ee/c4ee02853h#!divAbstract>
<https://doi.org/10.1039/C4EE02853H>
- [23] Meyer, K., Bashir, S., Llorca, J., Idriss, H., Ranocchiari, M. and Bokhoven, J.A. (2016) Photocatalyzed Hydrogen Evolution from Water by a Composite Catalyst of NH₂-MIL-125(Ti) and Surface Nickel(II) Species. *Chemistry—A European Journal*, **22**, 13894-13899.
<http://onlinelibrary.wiley.com/doi/10.1002/chem.201601988/abstract>
<https://doi.org/10.1002/chem.201601988>
- [24] Rimoldi, M., Howarth, A.J., DeStefano, M.R., Lin, L., Goswami, S., Li, P., Hupp, J.T. and Farha, O.K. (2017) Catalytic Zirconium/Hafnium-Based Metal-Organic Frameworks. *ACS Catalysis*, **7**, 997-1014.
<http://pubs.acs.org/doi/abs/10.1021/acscatal.6b02923?journalCode=accacs>
<https://doi.org/10.1021/acscatal.6b02923>
- [25] Shen, L., Liang, S., Wu, W., Lianga, R. and Wu, L. (2013) CdS-Decorated UiO-66(NH₂) Nanocomposites Fabricated by a Facile Photodeposition Process: An Efficient and Stable Visible-Light-Driven Photocatalyst for Selective Oxidation of

Alcohols. *Journal of Materials Chemistry*, **1**, 11473-11482.

<http://pubs.rsc.org/en/content/articlelanding/2013/ta/c3ta12645e#!divAbstract>

<https://doi.org/10.1039/c3ta12645e>

- [26] Ke, F., Wang, L. and Zhu, J. (2015) Facile Fabrication of CdS-Metal-Organic Framework Nanocomposites with Enhanced Visible-Light Photocatalytic Activity for Organic Transformation. *Nano Research*, **8**, 1834-1846.

<http://link.springer.com/article/10.1007/s12274-014-0690-x>

<https://doi.org/10.1007/s12274-014-0690-x>

- [27] Abedi, S. and Morsali, A. (2014) Ordered Mesoporous Metal-Organic Frameworks Incorporated with Amorphous TiO₂ as Photocatalyst for Selective Aerobic Oxidation in Sunlight Irradiation. *ACS Catalysis*, **4**, 1398-1403.

<https://doi.org/10.1021/cs500123d>



Scientific Research Publishing

Submit or recommend next manuscript to SCIRP and we will provide best service for you:

Accepting pre-submission inquiries through Email, Facebook, LinkedIn, Twitter, etc.

A wide selection of journals (inclusive of 9 subjects, more than 200 journals)

Providing 24-hour high-quality service

User-friendly online submission system

Fair and swift peer-review system

Efficient typesetting and proofreading procedure

Display of the result of downloads and visits, as well as the number of cited articles

Maximum dissemination of your research work

Submit your manuscript at: <http://papersubmission.scirp.org/>

Or contact mrc@scirp.org

